ACOUSTIC EMISSIONS AT AN OPEN CRACK

John A. Johnson

Idaho National Engineering Laboratory
EG&G Idaho, Inc.
P.O. Box 1625
Idaho Falls, ID 83415

Both finite difference and finite element techniques have been shown to be capable of modeling the propagation of acoustic emissions (AE) [1,2]. However, those calculations could also be done using the simpler Green's function methods [3]. In this work the finite element method is used to model a problem that includes complexities that cannot be handled using the Green's function methods.

In particular, the effect of the presence of a macrocrack on the received signal is investigated. We assume that the macrocrack interacts only as a geometric structure from which sound may reflect and mode convert, thereby complicating the signal at the receiving transducer. Numerical calculations of the AE field due to an open crack are compared to the Green's function results in a solid with no flaw.

FINITE ELEMENT CALCULATIONS

The computer program DYNA2D[4] was used to calculate the acoustic field due to a dipole force near the tip of a simulated crack. The calculation assumed a two-dimensional, plane-strain geometry. The surface-breaking crack was about halfway through the thickness of a 6.35-mm (0.25-in.) steel plate. This geometry is similar to that used in fracture tests of surface-crack specimens monitored with acoustic emission signals [5]. A dipole stress, perpendicular to the plane of the crack, was applied to the region near the crack tip, simulating the dynamic stress that would be present when the crack grows.

The grid is chosen to be made of quadrilateral elements about 0.2 mm on a side. The elements are square except in the region around the crack. The part is 32 elements thick; there are 73 elements to the right of the crack and 136 elements to the left. These last two distances were chosen so that a longitudinal wave from the crack would not reflect off the boundaries and return to a receiver 12.7 mm to the left of the crack.

The forcing function is chosen to have a Gaussian shape in time with a rise time of about 0.16 μs and a bandwidth of 3 MHz (20 dB). The minimum wavelength is then the shear wavelength, 1.07 mm, and the element size is less than one-fifth of this wavelength. The stress is also spread over three elements at the crack tip to prevent numerical noise.

The material properties are those of steel. The density is 7.8 g/cm^3. The moduli are chosen so that the sound speeds are 5.90 and 3.22 mm/μs for the longitudinal and shear velocities, respectively.

FINITE ELEMENT RESULTS

In Figure 1 the displacement field in the region around the crack tip as calculated by the program a short time after the force reaches its maximum amplitude is shown. The bottom of the part is at the bottom of the plot and the top of the part is not shown. In Figure 2 the displacement fields at 1, 2, and 3 μs are shown. In these plots the crack is in the lower left corner of the plot and only the region to the right of the crack is shown. At 1 μs the longitudinal wave is 4 mm from the crack tip. The shear wave can be seen in an arc starting at 5 mm on the vertical axis. The dominant feature is a surface wave which is traveling down the crack to 2 mm on the vertical axis. At 2 μs the longitudinal wave is centered between 9 and 10 mm in the horizontal direction. The head waves are clearly seen angling down behind the initial longitudinal wave. The many multiple reflections that have taken place by this time obscure most of the other individual wave modes except for the surface wave which has just turned the corner at the bottom of the crack. At 3 μs the surface wave is seen along the bottom horizontal axis between 3 and 4 mm, along with a reflection from the corner that has moved back up the crack and is near the tip in this snapshot. In Figure 3, the displacement field at 6 μs, the surface wave has moved along the bottom of the part to a point about 12 to 13 mm from the crack opening.

GREEN'S FUNCTION CALCULATIONS

A program provided by Hsu [3] was used to calculate the Green's functions for this case. The forcing function was a point dipole force located at the center of the distribution of forces used in the finite element calculation. This is not quite at the center of the part so that the calculated displacements at the same point on the top and bottom are slightly different.

Two time derivatives of the Green's function were calculated numerically since the input forcing function for the computation was a linear ramp. The second derivative was convolved in time with a filter function that had a bandwidth of half that of the forcing function in the finite element calculation. This provided an approximation to the filtering effect of the spatial distribution of the forcing function, in addition to the actual time dependence in the finite element calculation.

EFFECTS OF THE GEOMETRY OF THE CRACK

Now consider the effect of the crack on the received field at two points, on the top surface a distance of two thicknesses (12.7 mm, 0.5 in.) from the plane of the crack and on the bottom surface at the same distance. On the top surface the geometry of the crack is expected to have little effect. In Figure 4 the vertical displacement at the top-surface field point, as calculated by the Green's function and by the finite element program, is shown. The arrival of some of the larger modes can be identified and separated, and the waveforms are nearly the same. Some of the differences are due to the approximation of including the effect of the spatial distribution of the source in the time convolution. In particular the 3/2L (longitudinal wave that has traveled down from the source, reflected off the bottom, and traveled up to the field point on the top) and the 1/2SL (shear wave from the source to the bottom, mode converting to a longitudinal wave upon reflection which travels to the field point at the

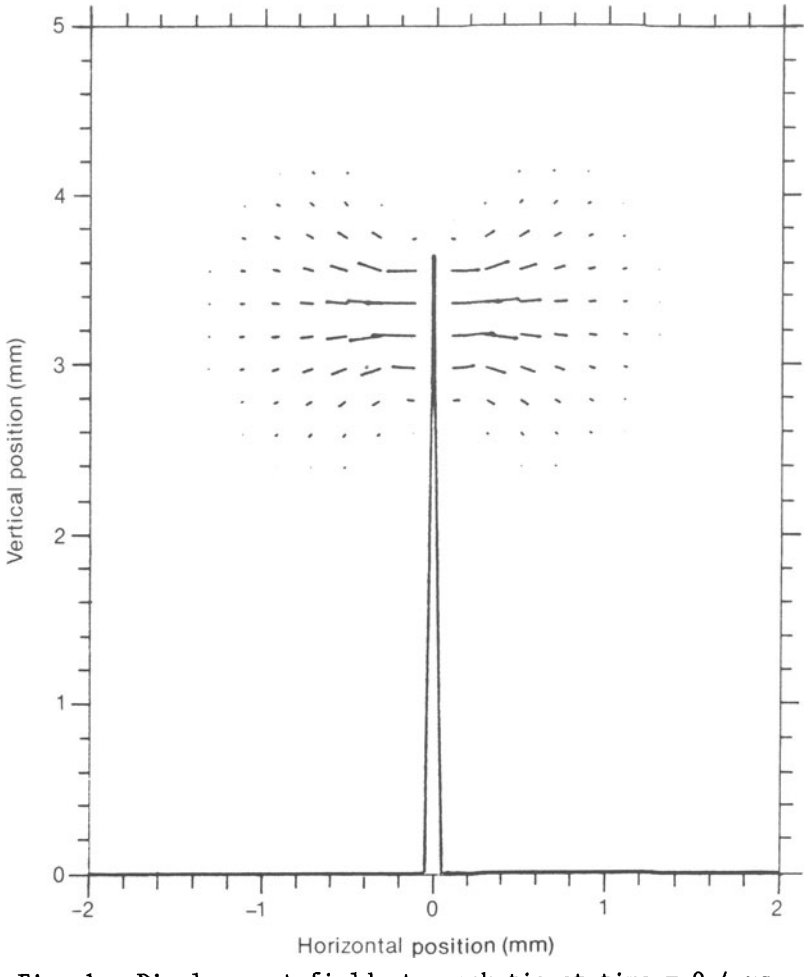

Fig. 1. Displacement field at crack tip at time = 0.4 μs.

top) are separate peaks in the Green's function but are not separated in the finite element calculation. Another difference is the two-dimensional, plane-strain approximation for the finite element calculation. This approximation probably causes the slight differences in timing of the arrival of the various modes. Finally, the crack may have some effect on the received signal, but the effect is relatively small.

In contrast, the same plots for the bottom of the part (Figure 5) show a marked difference, especially at the arrival time of the surface wave. Here the large positive peak in the convolved Green's function due to the arrival of the 3/2S mode is overwhelmed by the negative displacement due to the surface wave.

CONCLUSION AND FUTURE WORK

The finite element calculations which have been shown to be capable of correctly modeling acoustic emission signals have now been applied to a more complicated geometry which includes some of the effects of the crack. Further work needs to be done to incorporate effects neglected in these calculations, including the effect of asperities in the crack [6,7], and to extend the calculations to three dimensions.

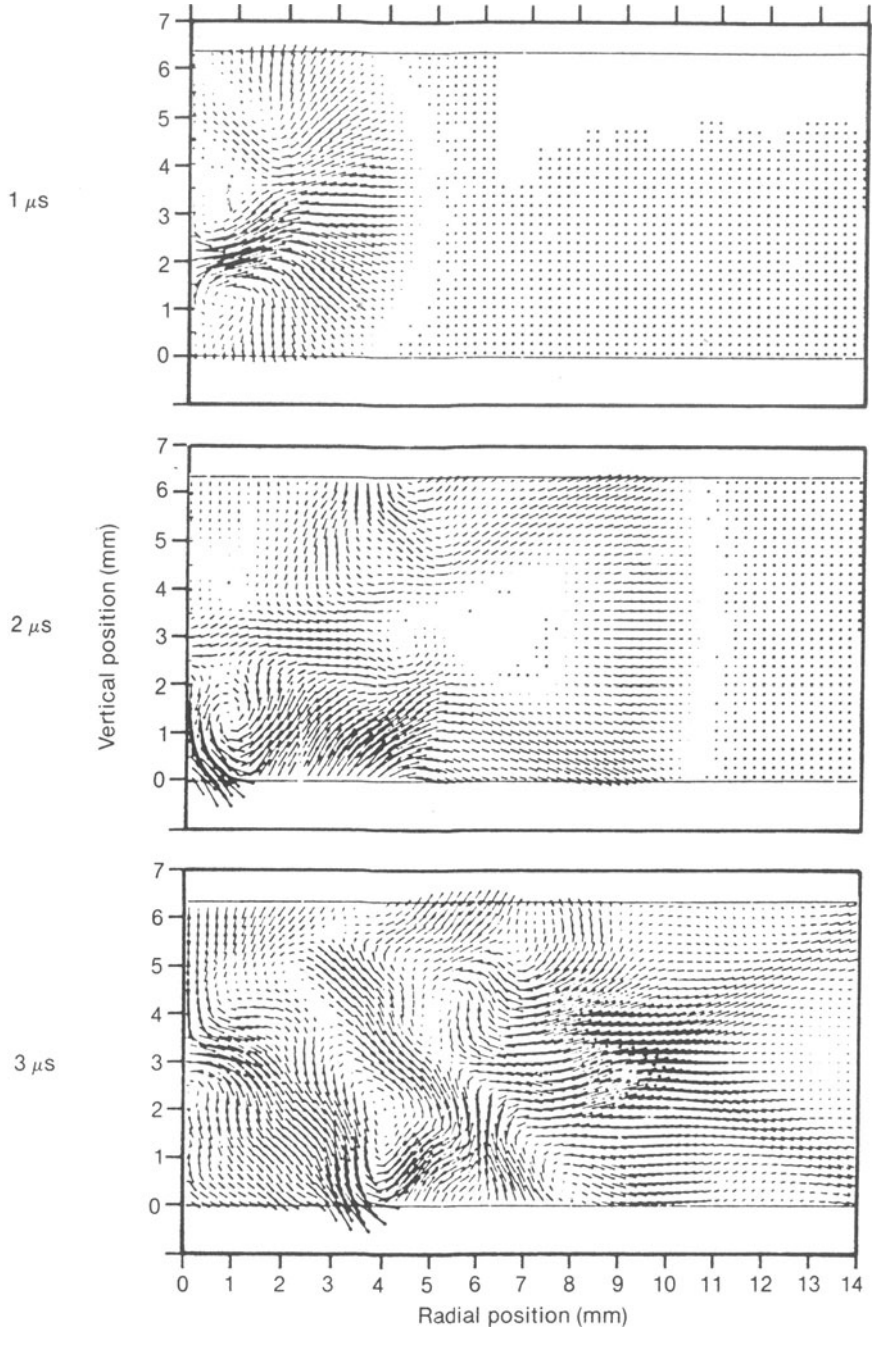

Figure 2. Displacement field at 1, 2, and 3 μs.

The potential use of these calculations is illustrated in Figure 6 where signals from a real acoustic emission event from a growing crack in an aluminum specimen are displayed. The specimen geometry is similar to that modeled in the finite element program. Four transducers are mounted on the specimen, two on the same side of the crack (Channels A and B) and two on

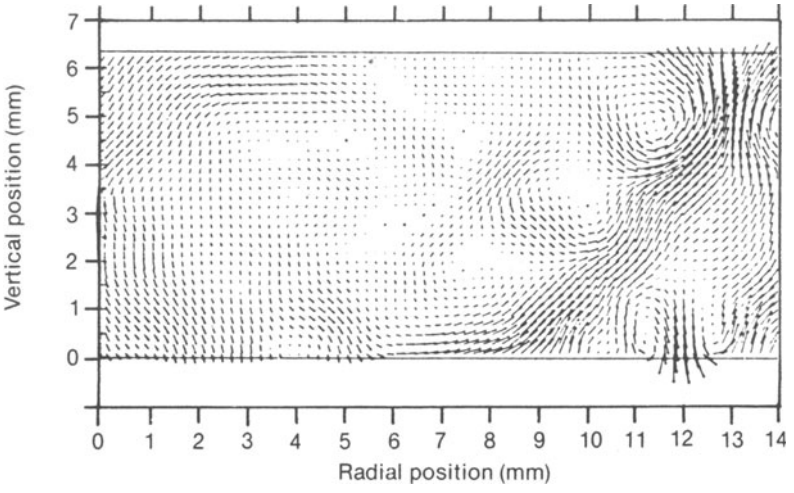

Figure 3. Displacement field at 6 μs.

the opposite side of the crack (Channels C and D). A distinct difference in the signals from the two sides can be seen, which is partially due to the effects seen in the finite element calculation.

In these experiments we desire to use acoustic emission for precise location and identification of the source. Using the beginning of the waveform for timing to determine location is difficult because of the small amplitude of the first arriving mode (longitudinal). If, through the study of the waveforms calculated using finite element techniques, a method of deconvolving out of the signal the arrival times of other modes could be developed (including surface waves traveling from the source along the crack), then more information would be available for locating the source. In addition, by modeling many different types of sources and comparing the results to the received signals, methods of source identification may be possible. Such analysis techniques would greatly reduce the cost and time required to do destructive analyses of these fracture specimens and would provide much more information, such as the relative time of the different events during the growth of a crack.

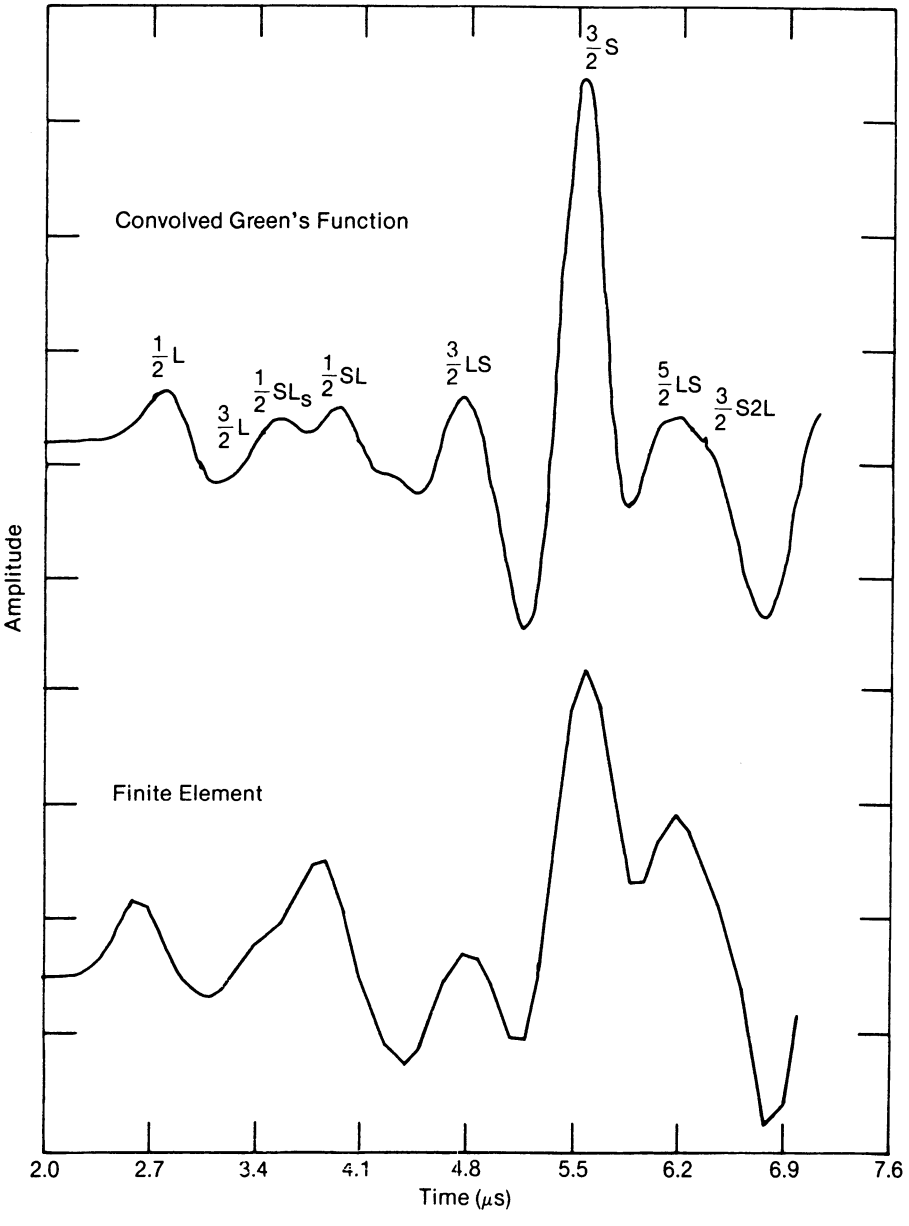

Fig. 4. Comparison of the porosity along the common line scan of the SiC sample from the optical measurements and the velocity and radiographic density calculations.

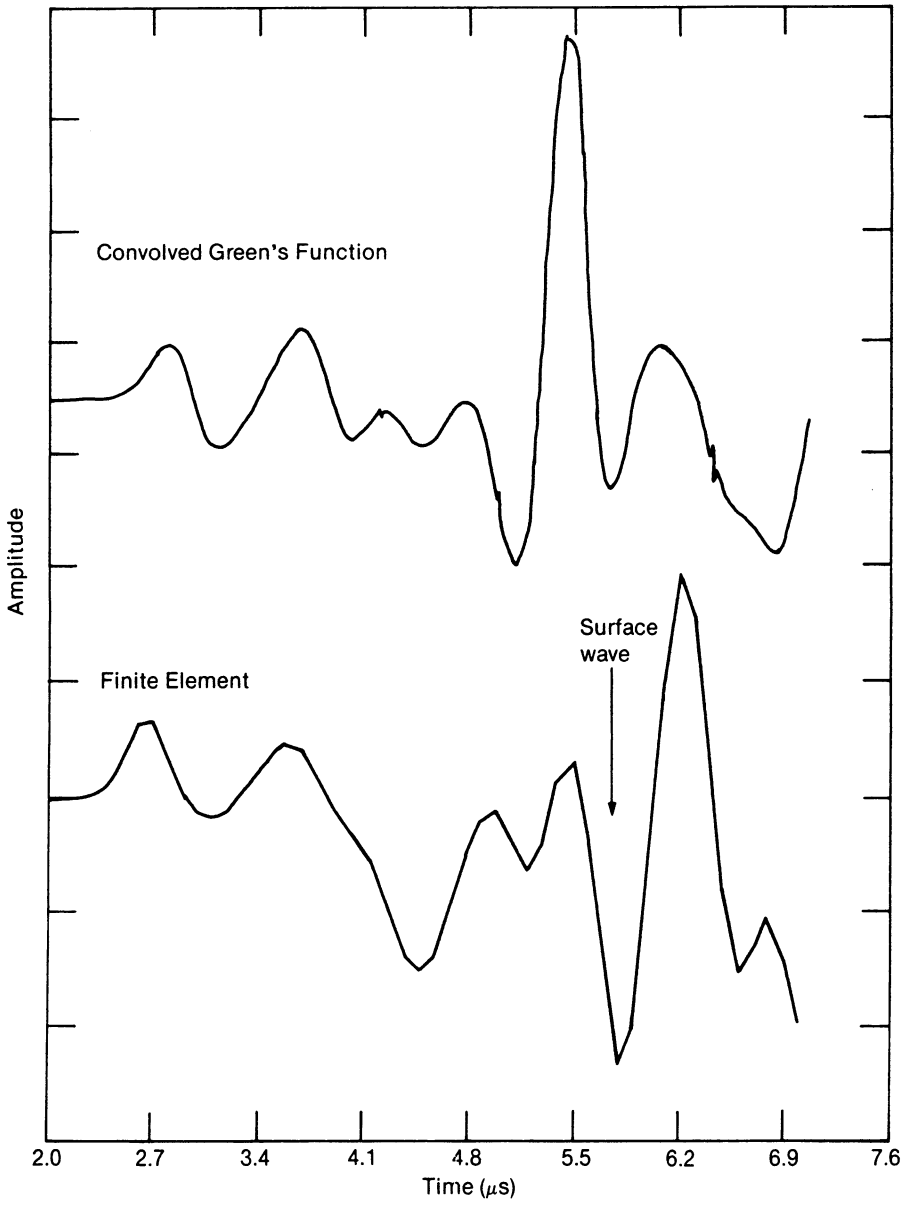

Fig. 5. Comparison of the detected echo decay patterns at positions A - E of the velocity curve in Fig. 2 along the common line scan of the SiC sample.

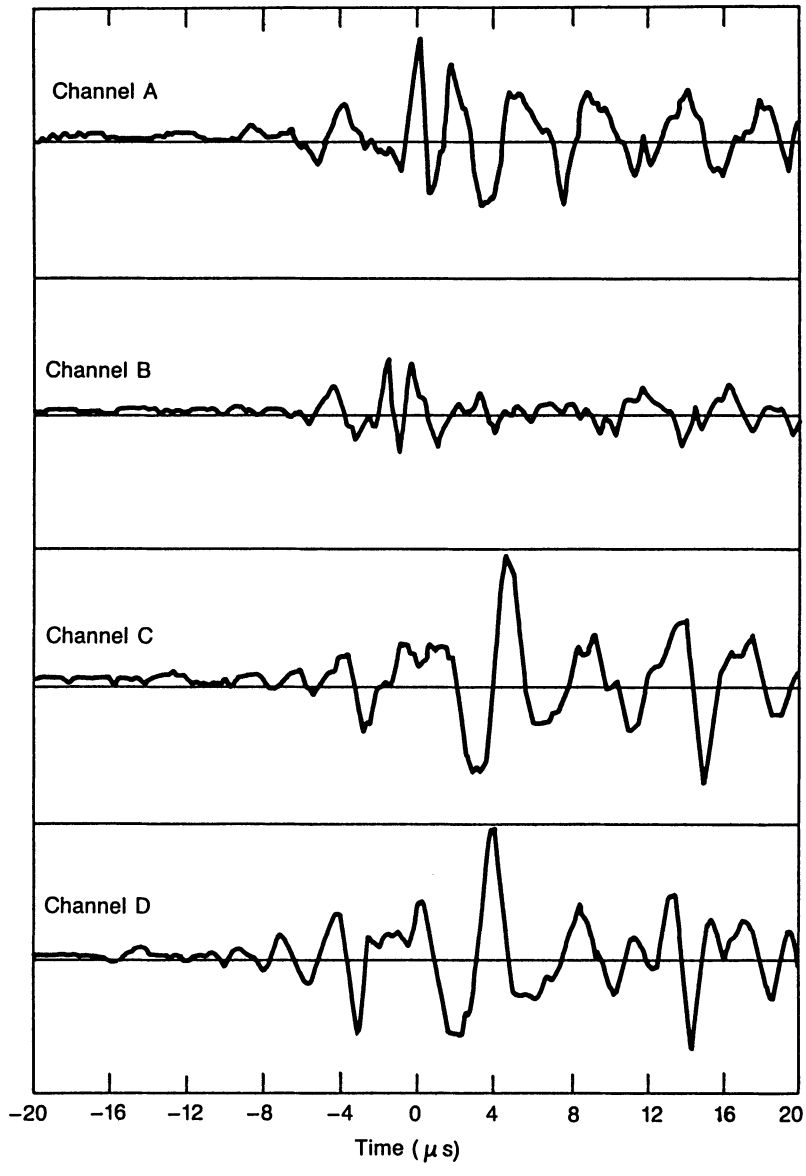

Fig. 6. Normalized plots of the first three echo energies for the SiC sample. The energies are normalized so that all echoes at the reference point (10 mm directly below the sample center) have the same value.

ACKNOWLEDGMENTS

This work is supported by the U.S. Department of Energy, Office of Energy Research, Office of Basic Energy Sciences under DOE Contract No. DE-AC07-76ID01570.

REFERENCES

1. J. A. Johnson, "Numerical Calculations of Acoustic Emission Signals," submitted to J. Acous. Soc. Am.

2. J. A. Johnson, "Numerical Calculations of Acoustic Emission Signals," Proceedings of the Review of Progress in QNDE 6, edited by D. O. Thompson and D. E. Chimenti (Plenum Press, New York, 1987).

3. N. N. Hsu, "Dynamic Green's Functions of an Infinite Plate - A Computer Program," National Bureau of Standards Report NBSIR 85-3234, August 1985.

4. J. O. Halquist, "User's Manual for DYNA2D - An Explicit Two-Dimensional Hydrodynamic Finite Element Code with Interactive Rezoning," Lawrence Livermore Laboratory Report UCID-18756 (Rev. 2), (1984).

5. B. A. Barna, J. A. Johnson, and R. T. Allemeier, "Determination of Crack Initiation Sites Using a Digital Acquisition Workstation," to be published in Experimental Mechanics.

6. R. B. Thompson and C. J. Fiedler, "The Effects of Crack Closure on Ultrasonic Scattering Measurements," Review of Progress in QNDE 3, edited by D. O. Thompson and D. E. Chimenti (Plenum Press, New York, 1984), pp. 207-215.

7. M. Punjani and L. J. Bond, "Scattering of Plane Waves by a Partially Closed Crack," Proceeding of the Review of Progress in QNDE 5, edited by D. O.Thompson and D. E. Chimenti (Plenum Press, New York, 1986), pp. 61-71.